Mechanical Removal and Rescreening of Local Screening Charges at Ferroelectric Surfaces

Sheng Tong (□□), Woon Ik Park, Yoon-Young Choi, Liliana Stan, Seungbum Hong, and Andreas Roelofs

Phys. Rev. Applied **3**, 014003 — Published 20 January 2015

DOI: 10.1103/PhysRevApplied.3.014003

Mechanical Removal and Rescreening of Local Screening Charges on Ferroelectric Surfaces

Sheng Tong (童盛)[1], Woon Ik Park[2], Yoon-Young Choi[2], Liliana Stan[1], Seungbum Hong[2,*], and Andreas Roelofs[1,*]

[1]*Nanoscience and Technology Division, Argonne National Laboratory, Lemont, IL 60439, USA*

[2]*Materials Science Division, Argonne National Laboratory, Lemont, IL 60439, USA*

ABSTRACT

We report the kinetics of screening charge removal and rescreening on periodically poled lithium niobate using charge gradient microscopy (CGM) and electrostatic force microscopy (EFM). A minimum pressure needs to be applied to initiate mechanical screening charge removal, and increasing the pressure leads to further removal of charge until a threshold is reached when all screening charges are removed. We fit all rescreening EFM contrast curves under various pressures into a universal exponential decay. The findings imply that we can control the screening degree of ferroelectric surfaces by mechanical means without affecting the polarization underneath.

KEYWORDS: electrostatic force microscopy, piezoresponse force microscopy, charge gradient microscopy, ferroelectric surface, kinetics of adsorption

---

* Corresponding authors: hong@anl.gov (S. H.) and aroelofs@anl.gov (A. R.)

Screening charges shield the electric field from the unbalanced bound polarization charges or other trapped charges until they are completely compensated. They are of great importance in many systems like piezoelectric actuators, ferroelectric thin films, colloid suspensions, solar batteries, and semiconductor devices [1-6]. In ferroelectrics, open circuit surfaces reach the ground state by either surface relaxation (internal screening) or adsorption (external screening). Internal screening will only be observed in ultrahigh vacuum and for most applications ambient conditions lead to external screening. For example, the adsorption on oxide surfaces can be tuned by polarization switching [4, 5], and on the other hand the chemical environment can control the ferroelectric polarization orientation [6].

In order to characterize the screening charges and the underlying polarization charges of ferroelectric materials, piezoresponse force microscopy (PFM), Kelvin probe force microscopy (KPFM), and electrostatic force microscopy (EFM) are widely used [7, 8]. Up to date two different methods have been employed to manipulate screening charges on ferroelectric surfaces. The first is to vary the polarization by changing the temperature and making use of the pyroelectric properties [8, 9]. The second is to inject charges onto the ferroelectric surfaces by applying a bias *via* a conductive atomic force microscopy (AFM) probe [10, 11]. Consequently, EFM or KPFM was then used to monitor the local charge adsorption on the ferroelectric surface. Yet there are inherent issues in separating screening charges from polarization charges: it is known that the adsorption rate (k) is temperature dependent,[1] and applying a bias over the coercive voltage switches the ferroelectric polarization and induces a depolarization field by injecting charges into the ferroelectric domains and domain walls [12, 13]. In addition, none of the methods can fully remove the screening charges and establish the fully unscreened state, which would be the "real" time zero in the adsorption kinetics [1]. We address this issue by

employing charge gradient microscopy (CGM), which can measures the displacement currents at the domain wall boundaries of the ferroelectrics in contact mode using a grounded conductive AFM probe (CGM probe), and efficiently remove screening charges by mechanical means and measure the collected charges during the process [14]. We demonstrate well-controlled mechanical removal of the external screening charges on the surface of a periodically poled lithium niobate (PPLN) and lead zirconate titanate (PZT) thin films, and investigate the rescreening kinetics subsequently.

To investigate the local screening charge removal and rescreening on the PPLN surface, we designed the experimental sequence as shown in Fig. 1a. First, we conducted an AFM and PFM scan to record the initial surface morphology and the ferroelectric domain configuration with a well-established method. The EFM scan is used to monitor the amount of screening before and after CGM scan. In a fully screened state, the variation of surface potential and surface potential gradient is much smaller than those in an unscreened state [8, 9, 15, 16]. Before the CGM experiment, the EFM signals did not show significant contrast as shown in Fig. 1d. After performing the CGM imaging (Fig. 1e), it is evident from the subsequent EFM measurement (Fig. 1f) that screening charges have been removed by the CGM scan and the stray electric fields are now detectable revealing the stripe domains in PPLN. The asymmetric EFM phase on positive and negative polarization domains may be due to the domain orientation dependent desorption energy [5, 6, 17, 18].

Figures 1g, 1h and S1 [19] prove that neither the topography nor the polarization of the PPLN has changed during the measurements. In order to study the screening charge removal process in more detail the CGM measurements have been repeated using a variety of different forces as well as scan speeds on the same area after the surface was again rescreened and no

EFM contrast was detected. Finally, an AFM and PFM measurement was conducted to confirm that the surface morphology and the ferroelectric polarization were unchanged. We corrected the sample drift, which occurred during the measurements by comparing the initial and final AFM and PFM images. Note that the dashed squares in Figs. 1b – 1h represent the CGM scanning area.

As shown in Figs. 1b and 1g, the initial and final topography showed no surface damage even though a pressure of up to ~450 MPa was applied, which is also seen in the line profiles in Fig. 1i before and after CGM. The average roughness (R_a) in Figs. 1b and 1g are 0.28 nm and 0.21 nm, respectively. In Fig. 1i, the current spikes of the CGM signal matched well with the PFM phase boundaries, e.g. positive polarity is observed where the PFM phase changed from 210° to 30°.

The contrasts in Fig. 1(f) further extend over the scanned range, which is due to the high speed of the CGM scanning and the way the AFM achieves reliable topography acquisition. The AFM scanner over-scans the range of the region set by the parameter we input to achieve the uniform speed in the scan range. Thus the outer acceleration and deceleration scanning leaves the wider domain patterns in the EFM image. One may note that such movement leaves wider domain patterns in the fast scan direction but not in the slow one.

More CGM experiments varying the number of lines in the slow scan axis over the same area did not reveal any significant difference in the CGM images. This indicates that the rate of charge removal is independent of the spacing over the range of line spacing we used. However, it should be noted that if the space between each line scan is much larger than the tip diameter, the width of removal is limited to the trace of the tip [20].

As shown in Fig. 2, we conducted a set of experiments on 90-nm-thick PZT (20/80) thin films deposited on $SrRuO_3/SrTiO_3$ substrates where the domain patterns were written during which excess charges were deposited to the PZT surface. Figs. 2a and 2b illustrate the smooth PZT films (R_a = 0.28 nm) consisted of bottom to top domains as deposited. After we wrote the +8 V and – 8V patterns, as in Fig. 2c, we observed the overscreened surface using EFM, similar to the previous reports [9, 10, 15, 21]. By conducting CGM on the same region (Fig. 2d), we observed using EFM the opposite charge polarity to that of the injected ones, which further confirmed that the surface charges were removed instead of created or injected.

The screening charges tend to neutralize the polarization charges of ferroelectric materials [8], as illustrated in Regime I of Fig. 3c, which minimizes the variation of surface potential above the stripe domains. Thus, the initial EFM phase image displays no contrast related to the domain pattern, indicative of surface potential variation resulting in smaller electric field gradient than the resolution of EFM. During the CGM imaging, we applied sufficiently large force to remove the screening charges without affecting the polarization underneath, leading to a strong potential gradient built up between up and down domains as shown in Regime III of Fig. 3. This is evidenced by the subsequent EFM image.

As we found that CGM could remove the screening charges from ferroelectric surfaces and detect the local surface potential gradients, we then further explored how the pressure applied to the probe and scan speed of the probe influence the rate of surface charge removal and the kinetics of rescreening.

Figure 3a shows the delta CGM current and EFM phase shift as a function of applied pressure. The EFM contrast ($\Delta\phi$) and CGM contrast (ΔI) vs. pressure (P) were plotted in Fig. 3a.

The contrast was defined as the difference between the maximum and minimum peaks, and the pressure was obtained by estimating hemispherical tip contact areas with a radius of 45 nm and 100 nm for the Pt-wired probe and Ir-coated Si probe, respectively. Figs. 3a can be divided into three regimes, marked by two parameters, the threshold pressure (P_{th}) and the critical pressure (P_{crit}): in Regime I where $P < P_{th}$, $\Delta\phi$ and $\Delta I \approx 0$, meaning that the CGM tip cannot remove screening charges; in Regime II where $P_{th} < P < P_{crit}$, $\Delta\phi$ and ΔI are proportional to the applied pressure P, implying that the CGM tip can partially remove screening charges and the removal rate is directly proportional to the applied pressure; in Regime III where $P > P_{crit}$, $\Delta\phi$ and ΔI are maximized, indicating that the screening charge was removed completely. The EFM phase shift is sensitive to the electric field gradient, which scales with the gradient of the net surface charges (ΔQ) for the same geometry [8, 15]. As we use stiff cantilevers, we can assume that $\Delta\phi$ scales linearly with ΔQ. As ΔI is proportional to the rate of ΔQ and the CGM scan speed was kept constant at 600 μm/s for all measurements, we expected that ΔI scales linearly with $\Delta\phi$, which is confirmed in Fig. 3b. The above discussion suggests three distinct regimes for CGM measurements which are depicted in Fig. 3c: (I) below P_{th} no CGM current is detected as the polarization charge is fully screened and screening charges cannot be removed; (II) the CGM current scales with the applied pressure as the CGM tip partially removes the screening charges; (III) the CGM current is saturated once the tip can fully remove the surface charges.

We assume that the screening charges are fully removed at high pressure applied on the CGM probe during the scan for the following reasons. Firstly, as the surface potential scales with the degree of screening, the surface potential variation after CGM scans measured using KPFM after at least two minutes is ~2.4 V on PPLN (Fig. S2) [19], which is 6 times larger than fully

screened surface [8, 9]. Secondly, we have showed [14] that the scraped charges per area are close to $2P_r$, indicating that we are scraping most, if not all, of the screen charges on the surface.

Time dependent EFM measurements were carried out to investigate the rescreening process after CGM scans. Figure 4a shows the dependence of $\Delta\phi$ decay as a function of time on the applied pressure. At time 1 min, $\Delta\phi$ strongly depends on the applied pressure, where a larger pressure is associated with a larger $\Delta\phi$. However, $\Delta\phi$ reached a minimum after about 7 min where $\Delta\phi$ was almost the same regardless of the initial applied pressure during the CGM measurement.

To quantify the kinetics of the rescreening, as shown in Fig. 4b, we approximated the time dependence of EFM contrast using an exponential decay function based on the following deductions. As the most polar composition in the atmosphere, water is the primary screening species [4, 16, 22]. By assuming that the rescreening is a first order adsorption, with the Elovich's equation and Lagergren's equation [23] as

$$\frac{d\theta}{dt} = k(1-\theta) \qquad (1)$$

where θ is the fraction of sites occupied by the charge carriers at time t (ferroelectric surface is unscreened at $t = 0$), k is the adsorption rate, we can integrate Eq. (1) to yield

$$1-\theta = \exp(-kt) \propto \sigma_{net} \qquad (2)$$

where σ_{net} is the net surface charge density. Since $\Delta\phi$ is proportional to σ_{net}, and k is the reciprocal of the adsorption half-life time τ, we can rewrite Eq. (2) to [9, 10, 15]

$$\Delta\phi = \Delta\phi_0 \exp\left(-\frac{t'}{\tau}\right) \quad (3)$$

where $t' = t - t_0$, $\Delta\phi_0$ is a prefactor, and t_0 is a time constant. The t_0 is not negligible when the screening charges are not fully removed, which is the case when $P_{th} < P < P_{crit}$. By fitting the two independent variables τ and t_0 for all the EFM contrast decay curves in Fig. 4a, we obtain a universal decay curve with τ of 2.37 min as seen in Fig. 4b. We also observed a similar value of τ of 2.18 min by directly monitoring the surface potential decay within a KPFM scan (Fig. S2) [19]. With the τ value in ~2 min, we can infer that the adsorption is chemical in nature with adsorption energy in tens to hundreds kJ/mol [1, 5, 17, 18, 23]. Usually, the screening process can be understood as follows: Firstly, the water is physisorbed to the ferroeletric surface in ps to ms; secondly, water is partially self-ionized into H_3O^+ and OH^-; and thirdly, the polar ions diffuse in surface water layer and electrostatically screen the polarization charges underneath in a few to tens of minutes [1, 15, 22, 24]. Because the physisorbed water does not screen the ferroelectric surface [1, 16-18], and physical desorption energy is much smaller than those of the chemisorbed H_3O^+ or OH^-, it is possible that not only the chemical bonding between the ions and polarization charges are broken mechanically but also the adsorbed water is pushed away due to the high scan speed during the CGM imaging.

We also considered other possible mechanisms such as mechanical wear or pressure induced surface piezoelectric potential that might lead to the same results we obtained. The simplest mechanism of removal of charged species is indeed the mechanical wear where the tip tears the chemical bond between the surface layer and the bulk of materials [25, 26]. We have observed the mechanical wear when we exerted 40 μN of loading force to the conductive diamond coated tip, where the topography of CGM area showed distinct indentation [14].

Regarding the possibility of pressure induced surface piezoelectric potential, we calculated that the charge induced by such a potential is at least two orders of magnitude lower than what we measured [14]. Therefore, although we cannot exclude the existence of the piezopotential, we believe it plays a minor role. Regarding the pressure effect on polarization dynamics, we note that those usually lead to non-volatile effect, such as flexoelectric effect induced polarization switching from one polarization to the opposite one or pressure induced phase transition from non-polar phase to polar phase [27, 28], which upon the removal of pressure will not return to the original state. However, in our case, as evidenced by Fig. 1, the periodically poled polarization pattern remained the same after the CGM imaging, which excludes those reversible but non-volatile effects.

The rescreening kinetics is strongly affected by the adsorbed molecule and ion species, temperature, and moisture, while our experiments were done in the ambient with no control over the humidity. Nevertheless, the universal τ under various applied pressure suggests that we remove the surface charges without perturbing the driving force for the rescreening, which is a function of both the ambient condition and the net charges from combination of the remaining screening charges, if any, and the polarization charges underneath. Noteworthy is that τ is different from the reported [9, 10], possibly due to the difference in the temperature and moisture, the state of screening (e.g. overscreening), and the type of the ferroelectric materials used in other studies.

As seen in Fig. 4b, a smaller P corresponds to a larger t_0, and *vice versa*. Based on Eq. (1), a bare ferroelectric surface is unscreened at $t = 0$, which implies that a finite t_0 corresponds to an effective elapsed time required for an unscreened surface to be rescreened to the initial screening state right after a CGM scan under a certain value of pressure (see Fig. S4) [19]. So

that a larger t_0 corresponds to a greater degree of screening and the value is determined by the applied pressure during the CGM scans.

From the discussion above, we have shown that the surface charges rescreened in a manner of an exponential recovery. A common τ regardless of the applied pressure implies a universal rescreening behavior, while the applied force determined the starting point in the decay curve. We also know that the applied force determines the amount of the charge removal from Fig. 3. Thus, based on the definition of t_0 and exponential recovery nature of the rescreening, we can define the degree of screening as

$$S = 1 - \exp\left(-\frac{t_0}{\tau}\right) \qquad (4)$$

where $S = 0$ for the unscreened surface, $S = 1$ for the fully screened surface. Similar to that of ΔI or $\Delta\phi$ vs. P in Fig. 3a, we find the plots of S *vs*. P in Fig. 4c. Obviously we again find the three regimes: in Regime I where $P < P_{th}$, $S \approx 0$; in Regime II where $P_{th} < P < P_{crit}$, S linearly decreased with the increase of P; in Regime III where $P > P_{crit}$, $S = 0$. By adopting the Eq. (3) and (4), we can quantitatively determine S, and thus precisely control the amount of the charge removal during the CGM scan.

Figure 5 displays the influence of scan speed of CGM on the screening charge removal process. The EFM phase images in Fig. S5 [19] implies that the total amount of the removed screen charge is the same, as shown in Fig. 5a. Therefore, the amount of the charges collected by AFM tip should linearly scale with the scan rate, which was confirmed in Fig. 5a [14]. The EFM contrast remains the same regardless of scan speed, however, varied with the applied pressure as

shown in Fig. 5b. This implies that the amount of charges removed by CGM probe is determined rather by the applied pressure and not primarily by the scan speed.

In summary, we studied the local surface charge removal and rescreening on PPLN surface using a CGM probe. We found that the applied pressure is the primary factor that determines the amount of the removed screening charges while the CGM scan-speed plays a minor role. The charge flow through the CGM probe is proportional to the magnitude of the removed screening charges. Unscreened polarization charges, which are exposed to the ambient, were rescreened in a matter of minutes following an exponential recovery with a universal half-life time τ of 2.37 min. These findings indicate that, with little impact on the ferroelectric polarization, we can control the degree of screening on a ferroelectric surface by mechanical manner. Furthermore, our work opens up an interesting field of mechano-chemistry and its dynamics at the nanoscale, which can lead to tunable surface chemistry by creating metastable charge state using local mechanical means.

ACKNOWLEDGMENT

The work was supported by the US Department of Energy, Office of Science, Materials Sciences and Engineering Division and by the Center for Nanoscale Materials, a US Department of Energy, Office of Science, Office of Basic Energy Sciences User Facilities under Contract DE-AC02-06CH11357. The work of EFM, PFM, and CGM was performed at Materials Science Division, and the work of SEM and PZT thin film deposition was performed at Center for Nanoscale Materials.

References

[1] A. W. Adamson and A. P. Gast, *Physical Chemistry of Surfaces* (Wiley-Interscience, the University of Michigan, 1997), p. 808.

[2] M. Grätzel, Dye-sensitized solar cells, J. Photochem. Photobiol. **4**, 145 (2003).

[3] M. Lannoo, C. Delerue, and G. Allan, Screening in semiconductor nanocrystallites and its consequences for porous silicon, Phys. Rev. Lett. **74**, 3415 (1995).

[4] Y. Yun and E. I. Altman, Using ferroelectric poling to change adsorption on oxide surfaces, J. Am. Chem. Soc. **129**, 15684 (2007).

[5] K. Garrity, A. M. Kolpak, S. Ismail□Beigi, and E. I. Altman, Chemistry of ferroelectric surfaces, Adv. Mater. **22**, 2969 (2010).

[6] R. V. Wang, D. D. Fong, F. Jiang, M. J. Highland, P. H. Fuoss, C. Thompson, A. M. Kolpak, J. A. Eastman, S. K. Streiffer, and A. M. Rappe, Reversible chemical switching of a ferroelectric film, Phys. Rev. Lett. **102**, 047601 (2009).

[7] S. Hong, *Nanoscale phenomena in ferroelectric thin films*, edited by S. Hong (Springer, USA, 2004), p. 288.

[8] S. V. Kalinin and D. A. Bonnell, Local potential and polarization screening on ferroelectric surfaces, Phys. Rev. B **63**, 125411 (2001).

[9] S. V. Kalinin and D. A. Bonnell, Screening phenomena on oxide surfaces and its implications for local electrostatic and transport measurements, Nano Lett. **4**, 555 (2004).

[10] Y. Kim, M. Park, S. Bühlmann, S. Hong, Y. K. Kim, H. Ko, J. Kim, and K. No, Effect of local surface potential distribution on its relaxation in polycrystalline ferroelectric films, J. Appl. Phys. **107**, 054103 (2010).

[11] X. Q. Chen, H. Yamada, T. Horiuchi, K. Matsushige, S. Watanabe, M. Kawai, and P. S. Weiss, Surface potential of ferroelectric thin films investigated by scanning probe microscopy, J. Vac. Sci. Tehcnol. B **17**, 1930 (1999).

[12] A. Roelofs, N. A. Pertsev, R. Waser, F. Schlaphof, L. M. Eng, C. Ganpule, V. Nagarajan, and R. Ramesh, Depolarizing-field-mediated 180^{o} switching in ferroelectric thin films with 90^{o} domains, Appl. Phys. Lett. **80**, 1424 (2002).

[13] S. Bühlmann, E. Colla, and P. Muralt, Polarization reversal due to charge injection in ferroelectric films, Phys. Rev. B **72**, 214120 (2005).

[14] S. Hong, S. Tong, W. Park, Y. Hiranaga, Y. Cho, and A. Roelofs, Charge gradient microscopy, Proc. Natl. Acad. Sci. USA. **111**, 6566 (2014).

[15] S. V. Kalinin, C. Johnson, and D. A. Bonnell, Domain polarity and temperature induced potential inversion on the $BaTiO_3$ surface, J. Appl. Phys. **91**, 3816 (2002).

[16] A. Ievlev, S. Jesse, A. Morozovska, E. Strelcov, E. Eliseev, Y. Pershin, A. Kumar, V. Y. Shur, and S. Kalinin, Intermittency, quasiperiodicity and chaos in probe-induced ferroelectric domain switching, Nature Phys. **10**, 59 (2014).

[17] D. Li, M. Zhao, J. Garra, A. M. Kolpak, A. M. Rappe, D. A. Bonnell, and J. M. Vohs, Direct in situ determination of the polarization dependence of physisorption on ferroelectric surfaces, Nature Mater. **7**, 473 (2008)

[18] J. Garra, J. M. Vohs, D. A. Bonnell, the effect of ferroelectric polarization on the interaction of water and methanol with the surface of $LiNbO_3$ (0001), Surf. Sci. **603**, 1106 (2009)

[19] See Supplemental Material at [URL will be inserted by publisher] for detailed experimental procedure, PFM amplitude images of PPLN before and after CGM scan, EFM and KPFM

images of the time dependent rescreening on PPLN surface, CGM scan speed influence on the EFM phases of PPLN surface, and more.

[20] Y. Kim, J. Kim, S. Bühlmann, S. Hong, Y. K. Kim, S.-H. Kim, and K. No, Screen charge transfer by grounded tip on ferroelectric surfaces, Phys. Status Solidi. (RRL) **2**, 74 (2008)

[21] J. Kim, Y. Kim, K. No, S. BÜHLMANN, S. Hong, Y. Nam, and S. Kim, Surface potential relaxation of ferroelectric domain investigated by kelvin probe force microscopy, Integr. Ferroelectr. **85**, 25 (2006).

[22] F. Verniani, The total mass of the Earth's atmosphere, J. Geophys. Res. **71**, 385 (1966).

[23] M. Low, Kinetics of Chemisorption of Gases on Solids, Chem. Rev. **60**, 267 (1960).

[24] T. Morimoto, M. Nagao, and F. Tokuda, the relation between the amounts of chemisorbed and physisorbed water on metal oxides, J. Chem. Phys. **73**, 243 (1969).

[25] K.-H. Chung, Y.-H. Lee, D.-E. Kim, J. Yoo, and S. Hong, Tribological Characteristics of Probe Tip and PZT Media for AFM-Based Recording Technology, IEEE Trans. Magn. **41**, 849 (2005)

[26] K.-H. Chung, Y.-H. Lee, Y.-T. Kim, D.-E. Kim, J. Yoo, and S. Hong, Nano-tribological characteristics of PZT thin film investigated by atomic force microscopy, Surf. Sci. **201**, 7983 (2007)

[27] H. Lu, C. W. Bark, D. Esque de los Ojos, J. Alcala, C. B. Eom, G. Catalan, and A. Gruverman, Mechanical Writing of Polarization, Science **6**, 59 (2012)

[28] P. Zubko, G. Catalan, and A. K. Tagantsev, Flexoelectric Effect in Solids, Annu. Rev. Mater. Res. **43**, 387 (2013).

Figure Captions

FIG. 1. Mechanical removal of surface charges. (a) Schematic of experimental sequence; (b) and (g) initial and final topography images of PPLN; (c) and (h) initial and final PFM phase images; (d) and (f) EFM phase images measured before and after the CGM scan; (e) CGM current; (i) Line profile of height (b, g), EFM phase (f), CGM current (e), and PFM phase (h).

FIG. 2. Evidence for removal of the injected charges on PZT thin films using CGM. (a) PZT topography, (b) PFM phase before and (c) EFM phase after selective charge injection by biasing the tip with -8 V and 8 V. (d) CGM after the EFM measurement in (c). (e) EFM phase after CGM scan in (d). (f) PFM phase of the domain writing pattern.

FIG. 3. Effect of applied pressure on surface charge removal. (a) CGM contrast (ΔI) and EFM contrast ($\Delta\phi$) as a function of applied pressure (P); (b) Correlation between ΔI and $\Delta\phi$; (c) schematic illustration of surface charge removal and rescreening in different regimes of (I) fully screened surface, (II) partial screened surface, and (III) unscreened surface.

FIG. 4. Surface charge rescreening after mechanical removal. (a) $\Delta\phi$ decay after CGM scans under various pressures (P); (b) universal $\Delta\phi$ decay fitted using Eq. (3), and elapsed time (t_0) vs. P; (c) screened percentage (S) vs. P.

FIG. 5. Scan speed influence to local surface charge removal and current flow. (a) Scan speed dependent ΔI and $\Delta\phi$; (b) Scan speed dependent $\Delta\phi$ after CGM scans under various pressures.

Figures

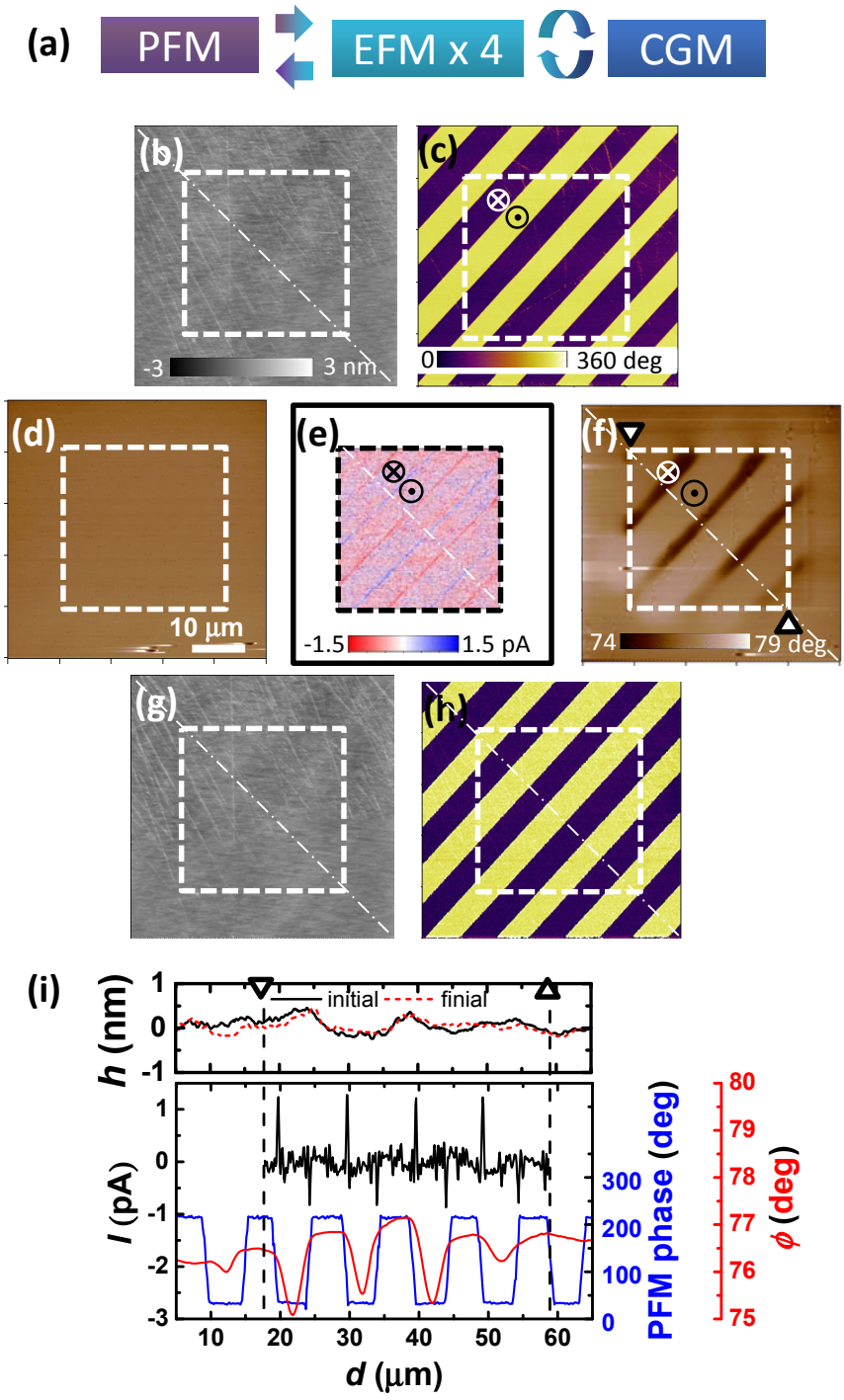

FIG. 1. S. Tong *et al*.

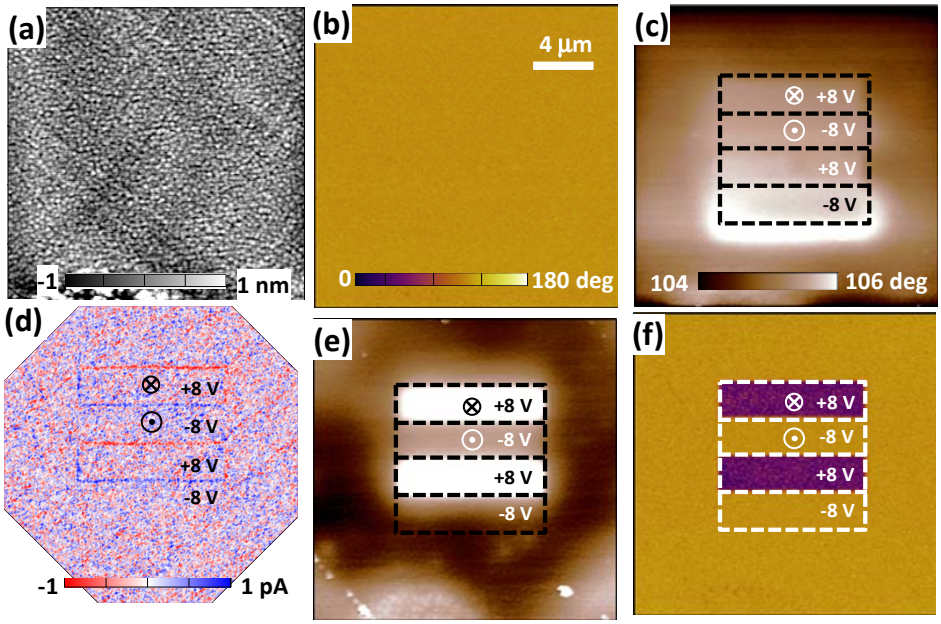

FIG. 2. S. Tong *et al*.

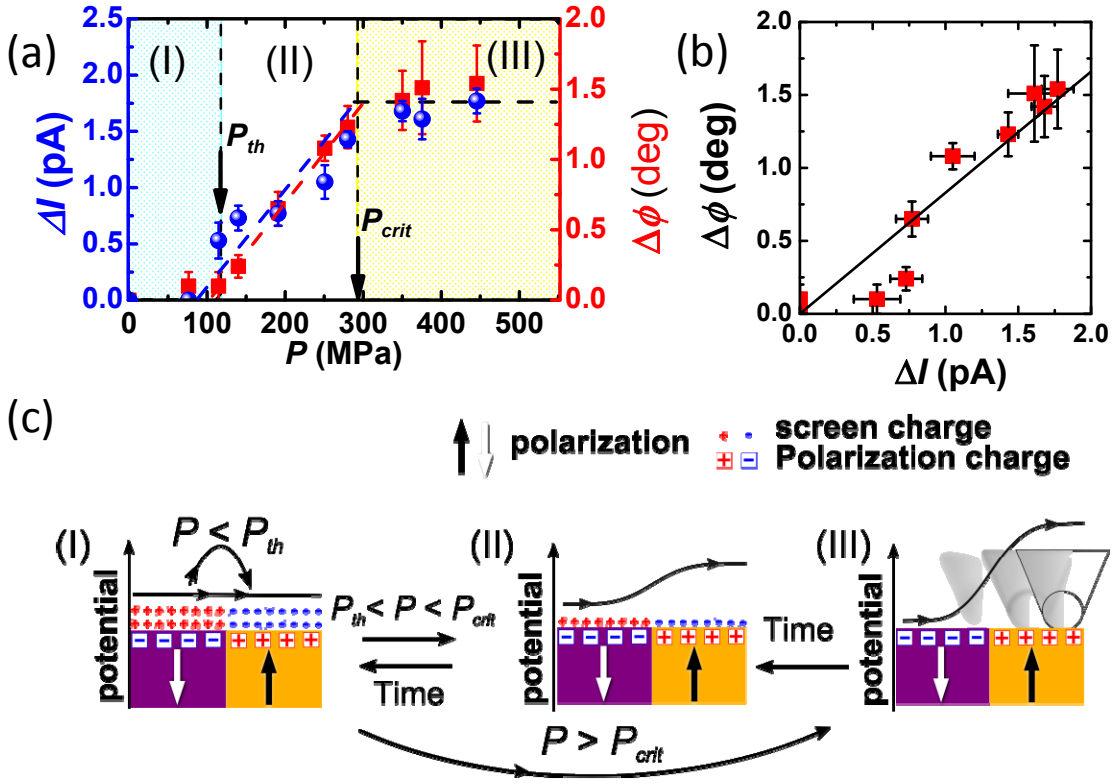

FIG. 3. S. Tong *et al*.

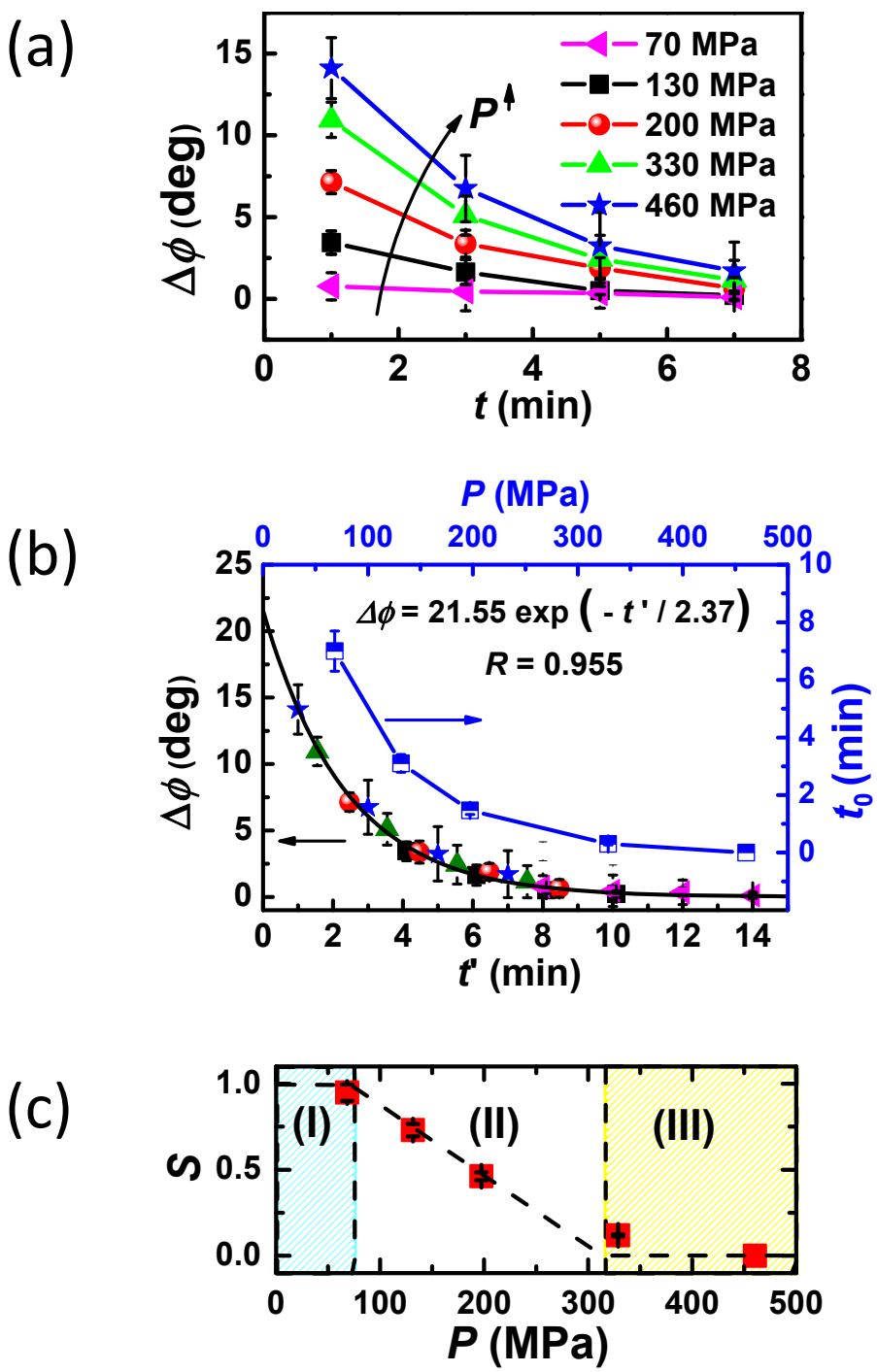

FIG. 4. S. Tong *et al*.

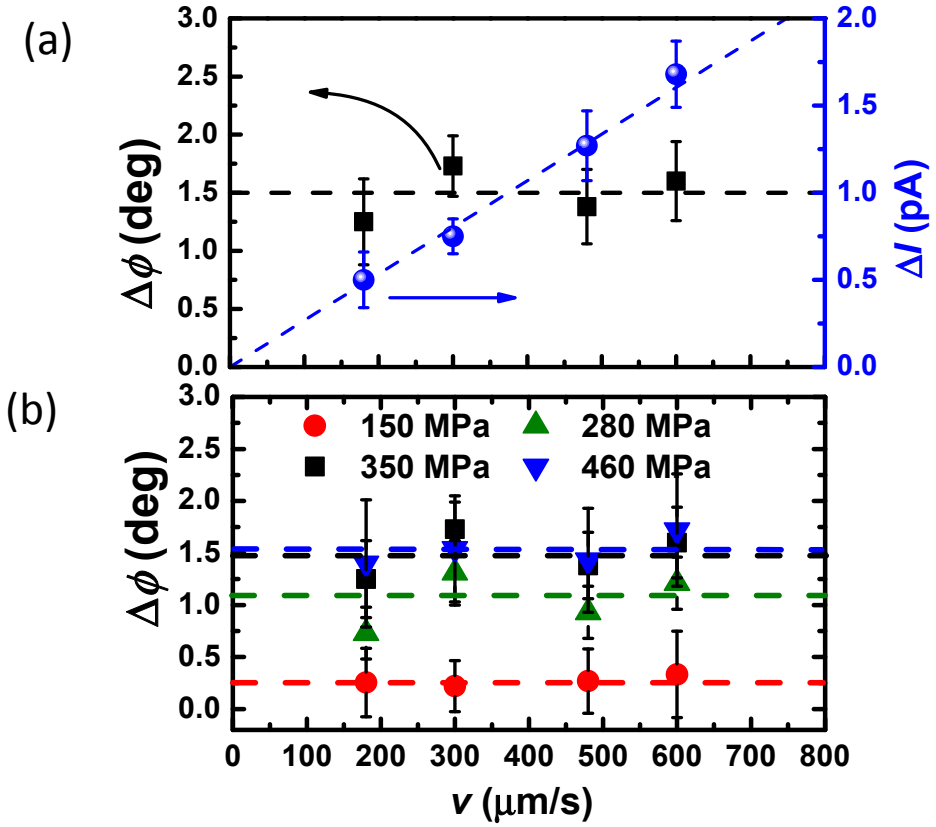

FIG. 5. S. Tong *et al*.